Published on *Ceramics International*, **30**,(6), 953-963, (2004) © by Elsevier Science Ltd.

The Influence of Microstructure on the Performance of White Porcelain Stoneware

P. M. Tenorio Cavalcante[a], M. Dondi[b], G. Ercolani[b], G. Guarini[b], C. Melandri[b], M. Raimondo[b], E. Rocha e Almendra[a]

[a]*UFRJ-COPPE, Federal University of Rio de Janeiro (Brasil)*

[b]*CNR-Institute of Science and Technology for Ceramics, via Granarolo 64, 48018 Faenza (Italy)*

Abstract
In the last years polished white porcelain stoneware tiles, coupling the smooth and glossy surface with the increased body whiteness, get a prominent role on the market. The bright white color is obtained by adding noteworthy quantity of opacifiers, such as zircon, corundum and spinel. The product microstructure, strictly dependent on the body formulation, has a decisive influence on the mechanical, tribological and functional behaviour of this class of products. To better understand these complex relationships, four polished white porcelain stoneware tiles were selected and thouroughly characterized by a wide spectrum of chemico-physical and microstructural analyses.

Keywords: D. Porcelain stoneware; A. Sintering; C. Mechanical properties; B. Microstructure

1. Introduction

Porcelain stoneware is a ceramic material with a very compact structure (water absorption <0.5%: group BIa of ISO 13006), made up of crystalline phases (new formed and residual ones) embedded in a glassy matrix, obtained by fast single firing (maximum temperature about 1200°C, less than 60 minutes cold to cold) [1, 2].
In the last decade, the growth rate of the global production of porcelain stoneware tiles increased more than other ceramic products; in fact, the excellent technical properties [3], together with the even more improved aesthetic appearance [4], gave porcelain stoneware a prominent role on the tile market [5]. This great commercial success made it possible to concentrate considerable resources in developing different types of porcelain stoneware tiles, which can be classified on the basis of their different surface or bulk properties. Both the surface (rough, textured, polished, lapped, glazed, etc) and the bulk appearance (i.e. translucency, whiteness, etc.) influence, though in a different way, the product performances [6, 7].
Among such different typologies, the last years recorded a significant advance in the production of polished tiles, having smooth and highly glossy surfaces compared to the untreated ones [8]. However, the occurrence of some drawbacks during the polishing procedures, mainly due to the opening of the closed porosity and formation of superficial flaws [9], leads to a worsening of the functional properties in working conditions, especially the resistance to stain [10,11] and the wear behaviour [12, 13].
Most studies available in the literature refer essentially to unglazed porcelain stoneware tiles, leaving significant opportunities for investigating the other typologies. In particular, the white porcelain stoneware, obtained by special body formulations able to get a bright white colour, is not fully investigated and a lot of aspects, from raw materials properties to processing conditions, should be better understood [14].

The white porcelain stoneware is obtained by special raw materials batches, containing low amounts of ball clays and kaolin (25-30%), high percentage of feldspars as fluxes (50-60%) and some quartz sands (5-10%). The increased whiteness, which gives added aesthetic value to the product, is achieved with a noteworthy quantity (5-15%) of opacifiers (zircon, corundum, spinel) [15, 16]. The microstructure of the fired products is strictly dependent on the particular body composition and has a decisive influence on the mechanical, tribological and functional behaviour of this class of products [2, 3].
In this standview, the behaviour of polished white porcelain stoneware tiles was thouroughly investigated by a wide spectrum of chemico-physical and microstructural analyses, focusing the attention on a better understanding of the complex relationships among microstructural, mechanical, tribological and functional characteristics. Besides the bulk properties, the surface state and their sensitivity to the wearing phenomena occurring in working conditions, have been also evaluated.

2. Materials and Methods

Four typologies of polished and unglazed white porcelain stoneware tiles, well representing the variability of the current production, were selected.
These products, named C, E, N and P respectively, were fully characterized in terms of compositional, microstructural, technological and functional properties.
The phase composition was quantitatively determined by X-ray powder diffraction (Rigaku Miniflex, Ni-filtered CuKα radiation) with the Reference Intensity Ratio method (CaF_2 as internal standard) [17]. The amount of glassy phase was estimated by difference. The experimental error is within 5% relative.
The chemical composition was determined by inductively coupled plasma – optical emission spectroscopy (ICP-OES, Varian Liberty 200) on the solution obtained by melting the sample with lithium tetraborate at 1200°C.
Open porosity and bulk density were quantified measuring the dry weight, the water-saturated weight and the weight suspended in water, according to ISO 10545-3. Total porosity was calculated by the ratio between bulk density and specific weight, measured by He pycnometer (Micromeritics Multivolume Pycnometer 1305); closed porosity was estimated by difference.
For each product typology, the modulus of rupture was measured with a 3-points flexural method (ISO 10545-4) on 7 to 10 tiles (400 x 400 mm^2 or 600 x 450 mm^2). An Instron 1195 instrument was used to determine the following mechanical properties on specimens cut off from commercial items: 4-points flexural strength (EN 843-1 on 45 x 4 x 3 mm^3 specimens), Young modulus (ENV 843-2 on 70 x 2 x 10 mm^3 specimens), as well as fracture toughness on 20 x 4 x 3 mm^3 bars with the single edge notched beam method (ENV 13234).
The surface microhardness was determined by a Zwick 3212 Vickers indenter (ENV 843–4, load of 0.3 kg), while the surface roughness, expressed as both R_a (average roughness) and R_t (maximum depression), was determined with a Taylor – Hobson instrument, according to CEN 85.
To simulate the wearing phenomena occurring on the tiles surface, both the PEI superficial wear resistance (ISO 10545-7) and the deep abrasion resistance (ISO 10545-6) were tested. The superficial resistance, measured after four wear steps (1500, 2100, 6000 and 12,000 rounds), is expressed as the volume of material removed from the surface converting the weight loss by the bulk density. The volume of material removed in the deep abrasion test is calculated by measuring the chord length of the groove.

The functional properties were evaluated in terms of surface stain resistance and cleanability, utilizing the red staining agent (Fe_2O_3 in a low molecular weight oil) and three different cleaning steps (WW: warm water, ND: warm water coupled with a neutral pH detergent, AD: warm water coupled with an abrasive alkaline pH detergent), according to ISO 10545-14. The staining after each cleaning step was appraised through a colourimetric measurement (ISO 10545-16, Hunterlab Miniscan XE Plus): the difference between the surface colour before and after the staining and cleaning operations is expressed as: $\Delta E = (\Delta L^{*2} + \Delta a^{*2} + \Delta b^{*2})^{1/2}$, where ΔL^*, Δa^* and Δb^* are the difference of the CieLab parameters L*, a* and b*, considering the as-received polished surface as reference.
The microstructure of the gold coated surfaces and cross-sections was also investigated through the SEM micrographies obtained with a Leica Cambridge Stereoscan 360 instrument. With the aim to locate the stress concentration areas, the crack sources and the preferred propagation patway, a fractographic analysis (ASTM C 1322) was also performed through SEM observations on the fractured surface originated during the 4-points mechanical tests.

3. Results and discussion

3.1. Chemical and phase composition

White porcelain stoneware tiles are produced with different body formulations; chemical data indicate several possible routes, all characterized by very low amounts of iron and titanium, together with a high content of ZrO_2 to achieve the lightest colouring (Table I). In most bodies, silica and alumina are around 68–69% and 17–19%, respectively, but alkaline oxides can be more o less abundant, predominantly sodic (body N) or sodic - potassic in similar amounts (bodies C and E). A completely different route is followed for body P: a relatively low amount of silica (58%) is coupled with high percentages of Al_2O_3 and ZrO_2, while, as fluxing, potassic oxide is prevaling over CaO and Na_2O.
The phase composition shows a certain variability of the amounts of both new formed and residual components (Table I). The amorphous phase is the most abundant component of the ceramic bodies, ranging from 49 to 58%. Quartz is the main crystalline phase, being in the range 21–26% in the silica–rich bodies, but just 9% in product P. Mullite reaches its maximum content in samples C and E (13–14%), while the amount of the residual plagioclase is up to 4%. Other residual phases are used as opacifying agent: the amounts of zircon and corundum are as high as 7–8% and 1–4% respectively, though zirconium silicate is significantly increased in sample P (about 14%).
The different amounts in terms of alkaline and alkaline-earth oxides of the bodies affect the formation and composition of the glassy phase, and hence its viscosity, surface tension and sintering behaviour (Table II) [17, 18]. The composition of the vitreous phase exhibits some features common to all samples, such as SiO_2 and Al_2O_3 values in rather strict ranges (67-72% and 13.5-14.7%, respectively) or the modest contents of iron and megnesium. The main differences concern the concentrations of sodium, potassium and calcium oxides: the glassy phase in the sample N is the richest in Na_2O, that in sample P is enriched in K_2O and CaO, while in sample C and E the vitreous component presents similar amounts of alkalis, though the sum $Na_2O + K_2O$ is higher in E. These chemical characteristics affect the viscosity of the liquid phase at high temperature (1200°C), which can be estimated about 0.9 MPa· s in the sodic glass of tile N, around 2-2.8 MPa· s in Na-K compositions (samples C and E) and approximately 3.5 MPa· s in the vitreous phase of sample P, where Na_2O, K_2O and CaO are present in notheworthy amounts [19, 20] .

In contrast, the values of surface tension are little influenced by chemical variations, ranging in all cases between 0.317 and 0.323 $N \cdot m^{-1}$ [18].

3.2. *Microstructure and physical properties*

Notwithstanding porcelain stoneware tiles are known for their enhanced compactness, the occurrence of a residual porosity, together with the presence of several crystalline phases - having different morphology and grain size - enclosed in a glassy matrix, involves the development of a very complex microstructure [2, 3].

Analysing the physical data, a total porosity ranging from 3.4 (sample N) to 6.0% (sample P), with a very small fraction belonging to open porosity (0.03–0.12%) was found. Bulk density is not strictly correlated with porosity values: sample P, in fact, exhibits the highest bulk density (2.51 g cm^{-3}), while samples C, E and N show very similar values (2.46–2.48 g cm^{-3}), not corresponding to their different porosity amounts (Table III). These apparent inconsistencies can be justified on the basis of the contribution of each phase to the bulk density. In particular, the presence in sample P of a greater amount of denser phases, such as zircon and corundum, can account for its higher density to porosity ratio [21].

The SEM micrographies reported in figure 1 reflect the porosity differences among samples C and N on one side, and sample E on the other side. The presence of a quite spherical porosity is also evident in samples C and E. Notwithstanding its highest total porosity, sample P presents a more compact microstructure, with pores having a smaller size and more irregular shape.

3.3. Mechanical properties

The flexural strength, calculated by the 3– and the 4–points methodologies, provides values ranging from 42 to 56 and 65 to 88 MPa, respectively. Young modulus varies from 69 to 77 GPa, while fracture toughness is between 1.14 and 1.31 $MPa \cdot m^{-0.5}$ (Table IV).

The mechanical resistance is positively correlated to (1-P) values, the only exception being sample N, whose lowest total porosity does not account for its worse performance (Figure 2). Respect to the 3–points resistance, the 4–points data are distributed in a wider range and correspond better to the porosity values differences. For this purpose, it is important to notice that with this latter methodology the local properties of the ceramic body can stand out, so that the presence of microstructural dishomogeneities, in terms of local defects and/or compressive stresses coming from the different properties of the mineralogical components, can act as flaws able to initiate a crack [22].

The elastic properties of the white porcelain stoneware bodies, expressed by the Young modulus, vary in a complex way with (1-P) values, so that no significant trend can be detected (Figure 2); the quite high resistance to elastic deformation presented by sample P is probably due to its phase composition, in particular to the greater amount of zircon and corundum, whose elastic moduli are higher than those of the other components [23]. As known, the elastic extension of a ceramic body is directly linked to the bonding forces and, considering that pore spaces should have approximately zero elasticity, the Young modulus is usually related well to both the body compactness and the structure energy [24, 25]. In the literature, some more o less satisfactory correlations of the bonding forces and the physical parameters with Young modulus (E) can be found [25]. For example, the following typical dependence of E on porosity (P) has been proposed:

$E = E_0 (1 - 1.9P + 0.9P^2)$, where E_0 is the elastic modulus of the pore-free ceramic body [26]. Nevertheless, these correlations work well for materials with the same structure (having, for example, an uniformly distributed porosity) and bond type. In a complex

multi–phase system, such as porcelain stoneware, Young modulus depends dramatically on the phase distribution and geometry, so that the correspondence with the proposed theoretical models is very difficult to find out [23]. The Young modulus of pore-free ceramics here considered, calculated from the contribution of each mineralogical component according to its weight fraction [21], confirms these difficulties: the E_0 value of sample P (83.3 GPa) can be explained by its high content of zircon and corundum; on the other hand, samples C and E exhibit a clearly different E_0 values (82.8 and 75.9 GPa, respectively) notwithstanding their similar phase composition.

As far as the fracture toughness, there is a significant positive correlation with (1-P) so that the higher the porosity, the lower the fracture toughness (Figure 2). According to the enhanced mechanical properties already mentioned, sample C exhibits the highest resistance to the fracture propagation as a consequence of a mechanical stress.

In the literature, the strength of porcelain ware is explained through three major theories [27-29]:

i) the mullite hypothesis (the interlocking of mullite needles is responsible for the enhanced strength) [30];
ii) the matrix reinforcement hypothesis (the differences in the thermal expansion coefficient between the glassy matrix and the dispersed crystalline particles produce strong compressive stresses with a consequent ceramic structure reinforcement) [31];
iii) the dispersion–strengthening hypothesis (the dispersed particles limit the size of Griffith flaws) [32, 33].

The mullite content of the samples here considered is generally related well to their mechanical resistance, calculated by both 3– and 4–points methodologies: the higher the mullite percentage, the higher the flexural strength, so that the “mullite hypothesis” seems to be effective (Figure 3).

The difference in thermal expansion coefficients between the glassy matrix (m) and the dispersed crystalline phases (p), as well as the Young modulus (E) and the Poisson’s ratio (ν) values, were utilized to calculate the total stress (P) on the particle, according to the following equation [27]:

$$P = \frac{\Delta\alpha\Delta T}{\left(\frac{1+\nu_m}{2E_m} + \frac{1-2\nu_p}{E_p}\right)}$$

where $\Delta\alpha$ is the difference in thermal expansion coefficients between the glassy matrix and the particle and Δ T the cooling range of the system. The occurrence and nature of cracks in porcelain bodies depend on the expansion coefficients differences: if the particle contracts more than the matrix, then P is negative and cracks around the particle can be found. On the contrary, if the matrix contracts more respect to the particle, then P is positive resulting in radial cracks emanating from the crystalline particle.

An attempt to apply this model to white porcelain stoneware was done taking the thermal expansion coefficients α in the 25-500°C range, Δ T = 500°C and the elastic moduli of each mineralogical component, as reported in table V. For each sample, the thermal expansion coefficient of the amorphous phase was calculated following the Appen’s mathematical model, though it was proposed in the 20-400°C range [34].

The P values obtained highlight that mullite and zircon undergo compressive stresses during cooling that, consequently, promote a material strengthening. In fact, when a crack front passes through a compressive stressed region, its propagation is contrasted if no additional external forces are applied. The calculated stress on the border of mullite particles is as high as 40 to 90 MPa approximately, while the P values

for zircon particles are much lower and pratically negligible (0.2-0.3 MPa) (Table VI). On the other hand, strong tensile stresses, in the order of 330-370 MPa, are developed around quartz particles, leading to a structural weakening and presumably a particle debonding from the matrix. According to these results, the toughening role played by mullite content is evident in samples C, E and P (Figure 3); however, sample N shows a quite high fracture toughness, notwithstanding its lowest mullite percentage.

The third strengthening hypothesis deals with the critical defect size (a_c) able to initiate the crack. The a_c values were calculated by the equation:

$$a_c = \left(\frac{Z}{Y}\right)^2 \left(\frac{K_{Ic}}{MOR}\right)^2$$

taking Y = 1.93 and Z = π /2 [35], K_{Ic} and MOR being the fracture toughness and the 4-points mechanical resistance data, respectively. This critical size of flaws is rather similar in all samples, ranging from about 140 to 200 μ m (Table III).

The fractographic analysis, performed with the aim to better locate the calculated stress distribution and the crack pathways, was unfortunately unable to reconstruct the sequence and cause of the fracture [36]. As a matter of fact, the typical fracture features were extremely difficult to be detected through the conventional SEM observations (Figure 4). Nevertheless, in some cases it was possible to point out the origin of the fracture, that seems attributable to superficial flaws (e.g. C, E and P in figure 4) or edge defects (i. e. sample E).

No flaw of a dimension analogous to the critical defect size was observed. Probably, the crack is caused by a coalescence of several dishomogeneities (pores, grains, etc.) smaller than 140-200 μ m [37]. This phenomenon depends to a large extent on the particular microstructure of porcelain stoneware, which can be considered as a composite microstressed material, where the presence of porosity, as well as of mineralogical components having a different reactive interface with the glassy matrix, determines a low energy fracture [29, 32, 37].

3.4. Tribological properties

The surface wear resistance was evaluated in terms of volume of material removed after superficial (60–73 mm^3) and deep abrasion (116–139 mm^3). Both these methodologies provide perfectly correlated data for samples C, E and P, while sample N shows a contradictory behaviour resulting as the most and the less resistant to superficial and deep abrasion, respectively (Table IV). A significant negative relationship comes out when the volume of abraded material is correlated with (1-P), with the anomalous data of sample N whose porosity does not account for its wear resistance (Figure 5). The Vickers microhardness of the other samples varies from 6.4 GPa of P to 6.8 GPa of E and C, roughly corresponding to the porosity scale; however, the surface hardness is clearly enhanced by mullite (Figure 6). In this case the behaviour of sample N is completely consistent with its lowest mullite percentage, which accounts also for its worse performance in the deep abrasion test. The narrower range of the results coming from the superficial abrasion seems to indicate a less pronounced dependence on the phase composition.

In the literature different models have been proposed in order to predict the amount of material removed per unit length (Q) during abrasion, such as that proposed by Hutchings [38]:

$$Q = k \frac{W^{5/4} d^{1/2}}{A^{1/2} K_{Ic}{}^{3/4} H^{1/2}}$$

where k is a material-independent variable, W is the applied load, d is the abrasive particle size, A is the apparent contact angle, K_{Ic} is the fracture toughness and H is the

Vickers microhardness. Taking into account the deep abrasion test, performed with W = 27.93 N and d = 0.185 mm, the values of Q and A listed in table 4 were obtained.
Applying the Hutching's model, a good correspondence between observed and predicted wear rates is found for samples C, E and P, while the sample N exhibits a wear ratio higher than expected on the basis of its fracture toughness and hardness (Figure 7).
For this purpose, it is important to point out that, in the wearing simulation tests of polished surfaces, the presence of surperficial damages, caused by the industrial machining procedure, can influence the results. In other words, the different processing parameters, adopted by each company during polishing and probably not completely controlled, induce the formation of scratches and flaws, whose amount and distribution can affect the Vickers data.

3.5. Functional properties

The industrial polishing procedure, to which tiles were subjected, allowed to significantly reduce the surface roughness, removing unevenness and asperities. The roughness decreasing depends one more time on the choice of machining procedure and parameters, but also on the microstructural features of the ceramic body. The average roughness (R_a) of the white porcelain stoneware bodies is in the 0.23-0.32 μ m range, while the maximum depression detected on the surface (R_t) can reach 9 μ m, as in the case of sample N (table IV). The surface roughness is inversely related to the hardness, while no clear relationship can be detected with the porosity.
In table IV, the colourimetric Δ E differences, referring to the staining and cleanability of the products, are listed. According with the three cleaning steps, the colourimetric differences are reported as Δ E (WW = warm water), Δ E (ND = neutral detergent), Δ E (AD = alkaline detergent). From the results obtained, the following conclusions can be drawn:

- the best cleanability of sample C is independent from the nature of the detergent used, showing a very good performance even if only warm water is used;
- samples P and E show a similar performances only after using neutral or abrasive detergents;
- the behaviour of sample N is quite different, having, in all conditions, the worse cleanability.

It is important to notice that the best functional properties shown by samples C, E and P, when compared to sample N, are directly linked to their lower value of both average and maximum roughness (figure 8). The worse stain resistance of sample N should be better analysed on the basis of the pores size and morphology, besides its porosity value, since its high R_t value probably involves the presence of bigger pores on the surface. In fact, the occurrence of pores at the working surface, together with the presence of scratches and cracks, allows stain agents to easily penetrate and, sometimes, depending on their different nature, it could be very hard to remove them.

4. Conclusions

White porcelain stoneware are tiles with an added value due to the enhanced aesthetic appearance, consisting in highly white and glossy surfaces obtained by polishing.
Different routes are followed in body design varying the relative amount of fluxing oxides, though body formulations always include zirconium silicate and/or alumina in considerable amounts as opacifiers. Phase composition consists of a glassy phase prevailing over residual quartz and feldspars, new formed mullite and opacifying additives (zircon and corundum). The chemical composition of the vitreous phase

changes from sample to sample; consequently, the viscosity of the liquid phase at higher temperatures and sintering kinetics vary upon the body formulation.
White porcelain stoneware tiles are characterized by a very low water absorption, though a residual closed porosity is present in significant amounts (3-6%) leading to a different compactness and microstucture. Products exhibit excellent mechanical properties: 65-88 MPa of flexural strength, 69-77 GPa of Young modulus, 1.1-1.3 $MPam^{0.5}$ of fracture toughness, with a clear dependence of these properties on porosity and phase composition. Mullite and zircon tend to increase the mechanical performances, through a predominant mechanism of matrix reinforcement, while quartz plays an opposite role.
White porcelain stoneware tiles have good wear resistance connected with a Vickers hardness ranging from 6.2 to 6.8 GPa. The behaviour in the deep abrasion test corresponds well to a prediction model based on both surface hardness and fracture toughness. The different products present a different stain resistance and cleanability, related to a) polishing and b) microstructure. The rougher the surface, the easier to stain and the hardest to clean, while a less compact microstructure allows to obtain better functional performance.

References

1. T. Manfredini, G. C. Pellacani, M. Romagnoli, L. Pennisi, Porcelainized stoneware tiles, Am. Ceram. Soc. Bull. 74 (5) (1995) 76-79.
2. M. Dondi, G. Ercolani, C. Melandri, C. Mingazzini, M. Marsigli, The chemical composition of porcelain stoneware tiles and its influence on microstructural and mechanical properties, Interceram 48 (1995) 75-83.
3. M. Dondi, B. Fabbri, T. Manfredini, G. C. Pellacani, Microstructure and mechanical properties of porcelainized stoneware tiles, in: Proceedings of the 4th Ecers, 1995, pp. 319-326.
4. L. Mucci, Topicality and prospects of increasing the aesthetic value of porcelain stoneware, Ceramurgia 20 (1) (1990) 20-23.
5. G. Biffi, Porcelain stoneware market in Europe: development and future forecasts, Ceramica Informazione 385 (34) (1999) 54-60.
6. J. Trpcevska, J. Briancin, L. Medvecky, Microstructure and porcelain stoneware properties, Key Engineering Materials 223 (2002) 265-267.
7. A. P. M. Menegazzo, J. O. A. Paschoal, A. M. Andrade, D. Gouvêa, J. C. Carvalho, Evaluation of the technical properties of porcelain tile and granite, in: Proceedings of Qualicer, 2002, pp. 211-230.
8. L. Esposito, A. Tucci, Porcelain stoneware tile surfaces, Am. Ceram. Soc. Bull. 79 (5) (2000) 59-63.
9. M.J. Orts, E. Sanchez, J. Garcia-Ten, M.J. Ibañez, J. Sanchez, C. Soler, J. Portoles, Comportamiento del gres porcelanico durante la operacion de pulido. Bol. Soc. Esp. Ceram. Vidrio 40 (6) (2001) 445-453.
10. L. Esposito, A. Tucci, E. Rastelli, C. Palmonari, S. Selli, Stain resistance of porcelain stoneware tiles, Am. Ceram. Soc. Bull. 81 (10) (2002) 38-42.
11. J. O. A. Paschoal, A. P. M. Menegazzo, F. L. N. Lemos, D. Gouvêa, R. S. N. Nóbrega, Study of porcelain tile stain resistance, in: Proceedings of Qualicer, 2002, pp. 213-215.
12. G. Silva, A. Munõz, C. Feliu, M. J. Ibañez, J. Barbera, C. Soler, Abrasion resistance of ceramic flooring in actual heavy traffic conditions, in: Proceedings of Qualicer, 2002, pp. 79-82.
13. A. Tucci, L. Esposito, L. Malmusi, A. Piccinini, Wear resistance and stain resistance of porcelain stoneware tiles, Key Engineering Materials 206-213 (2002) 1759-1762.
14. F. Ginés, A. Orenga, A. Sheth, D. Thiery, Use of spodumene for manufacturing porcelain tile bodies of high whiteness, in: Proceedings of Qualicer, 2002, pp. 47-50.
15. G. Baldi, E. Generali, D. Settembre Blundo, Preparazione, caratterizzazione ed applicazione industriale di un vetroceramico appartenente al sistema ZrO_2-CaO-SiO_2 (ZCS) come componente in impasti da gres porcellanato, Ceramurgia 30 (2000) 161-171.
16. V. Biasini, M. Dondi, S. Guicciardi, C. Melandri, M. Raimondo, E. Generali, D. Settembre Blundo, Mechanical properties of porcelain stoneware tiles: the effect of glass ceramic system, Key Engineering Materials 206-213 (2002) 1799-1802.
17. T. Lakatos, L-G. Johansson, B. Simmingsköld, Viscosity temperature relations in the glass system SiO_2-Al_2O_3-Na2O-K_2O-CaO-MgO in the composition range of technical glasses, Glass Technology 13 (3) (1972) 88-95.

18. F. Cambier, A. Leriche, Vitrification, Materials Science and Technology – A Comprehensive Treatment, Vol 17B, Processing of Ceramics, Part II, VCH, 1996.
19. G. Bonetti, Impostazioni matematiche per calcolare le proprietà dei vetri in funzione della composizione chimica. III parte: viscosità, Rivista della Stazione Sperimentale del Vetro (4) (1998) 175-190.
20. G. Bonetti, Impostazioni matematiche per calcolare le proprietà dei vetri in funzione della composizione chimica. IV parte: viscosità, Rivista della Stazione Sperimentale del Vetro (6) (1998) 271-286.
21. J. F. Shackelford, W. Alexander, Material Science and Engineering Handbook, Third Ed., CRC Press, 2001.
22. N. E. Dowling, Mechanical behavior of materials, Prentice-Hall Int. Ed. (1993).
23. W. D. Kingery, H. K. Bowen, D. R. Uhlmann, Introduction to Ceramics, Second Edition, John Wiley & Sons, Inc., New York, 1976.
24. A. R. Boccaccini, G. Ondracek, O. Postel, Module de Young de Céramiques Poreuses, Silicates Industriels 9, 10 (1994) 295-299.
25. A. S. Wagh, R. B. Poeppel, J. P. Singh, Open pore description of mechanical properties of ceramics, Journal of Materials Science 26 (1991) 3862-3868.
26. J. K. MacKenzie, Proc. Phys. Soc. (Lond) B63, 1950.
27. W. M. Carty and U. Senapati, Porcelain-Raw Materials, Processing, Phase Evolution, and Mechanical Behavior, J. Am. Ceram. Soc. 81 (1) (1998) 3-20.
28. S. Maity & B. K. Sarkar, Phase Analysis and Role of Microstructure in the Development of High Strength Porcelains, Ceramics International 24 (1998) 259-264.
29. C. Leonelli, P. Veronesi, V. Cannillo, G. C. Pellicani, A.R. Boccaccini, Porcelainized Stoneware as a Composite Material: Identification of Strengthening and Toughening Mechanisms, Tile & Brick Int. 17 (4) (2001) 238-244.
30. L. Mattyasovszky-Zsolnay, Mechanical strength of porcelain, J. Am. Ceram. Soc. 40 (1957) 299-306.
31. D. Weyl, Influence of internal strains on the texture and mechanical strength of porcelains, Ber. Deut. Keram. Ges. 36 (1959) 319-324.
32. L. Esposito, E. Rastelli, A. Tucci, A. Albertazzi, Porcelain Stoneware Matrix Composite: Aspects and Perspectives, Silicates Industriel 65 (1-2) (2000) 3-7.
33. S. Maity & B. K. Sarkar, Development of High-Strength Whiteware Bodies, J. Eur. Ceram. Soc. 16 (1996) 1083-1088.
34. G. Bonetti, Impostazioni matematiche per calcolare le proprietà dei vetri in funzione della composizione chimica. I: Massa volumica, dilatazione termica, Rivista della Stazione Sperimentale del Vetro (3) (1997) 111-125.
35. A. D. Papargyris, R. D. Cooke, Structure and mechanical properties of kaolin based ceramics, Br. Ceram. Trans 95 (3) (1996) 107-120.
36. ASTM C 1322, Fractography and Characterization of Fracture Origins in Advanced Ceramics,1996.
37. G. D. Quinn, J. J. Swab, Fractography and estimates of fracture origin size from fracture mechanics, Ceram. Eng. Sci. Proc. (3) (1996) 51-58.
38. I. M. Hutchings, Tribology: Friction and Wear of Engineering Materials, Edward Arnold, London, 1992.

Table I – Chemical and phase composition of white porcelain stoneware tiles

wt %	C	E	N	P
Mullite	14.4 ± 1.4	13.4 ± 1.5	8.8 ± 1.7	10.8 ± 1.3
Quartz	24.1 ± 0.9	21.4 ± 1.0	25.8 ± 0.5	8.8 ± 0.4
Cristobalite	0.4 ± 0.1	<0.1 ± 0.1	1.2 ± 0.1	1.0 ± 0.1
Plagioclase	0.7 ± 0.1	0.4 ± 0.1	4.0 ± 0.2	3.7 ± 0.1
Zircon	6.8 ± 0.8	6.6 ± 0.8	7.8 ± 1.1	13.6 ± 1.0
Corundum	0.7 ± 0.2	0.8 ± 0.1	3.6 ± 0.2	3.7 ± 0.4
Amorphous	52.0 ± 3.1	57.0 ± 2.9	48.9 ± 2.7	58.0 ± 2.2
SiO_2	68.89 ± 1.40	68.24 ± 1.50	68.65 ± 1.50	57.95 ± 1.30
TiO_2	0.38 ± 0.03	0.31 ± 0.02	0.42 ± 0.03	0.08 ± 0.01
ZrO_2	4.56 ± 0.30	4.40 ± 0.29	5.20 ± 0.31	8.78 ± 0.55
Al_2O_3	19.00 ± 0.67	19.23 ± 0.71	17.36 ± 0.58	20.70 ± 0.68
Fe_2O_3	1.11 ± 0.03	1.01 ± 0.03	0.40 ± 0.03	0.84 ± 0.02
MgO	0.42 ± 0.06	0.32 ± 0.05	0.43 ± 0.07	0.81 ± 0.12
CaO	0.67 ± 0.10	0.42 ± 0.07	0.38 ± 0.08	2.60 ± 0.30
Na_2O	2.49 ± 0.12	3.36 ± 0.17	4.99 ± 0.25	2.36 ± 0.12
K_2O	2.52 ± 0.10	2.99 ± 0.20	1.45 ± 0.18	4.55 ± 0.33
P_2O_5	0.07 ± 0.02	0.17 ± 0.10	0.09 ± 0.03	0.17 ± 0.10

Table II – Calculated chemical composition, viscosity and surface tension of the vitreous phase

wt %	C	E	N	P
SiO_2	71.8 ± 1.5	70.9 ± 1.4	70.9 ± 1.4	67.2 ± 1.3
TiO_2	0.7 ± 0.1	0.5 ± 0.1	0.9 ± 0.1	0.1 ± 0.1
Al_2O_3	14.0 ± 0.3	14.6 ± 0.3	13.5 ± 0.3	14.7 ± 0.3
Fe_2O_3	2.1 ± 0.1	1.8 ± 0.1	0.8 ± 0.1	1.5 ± 0.1
MgO	0.8 ± 0.1	0.6 ± 0.1	0.9 ± 0.1	1.4 ± 0.1
CaO	1.2 ± 0.1	0.7 ± 0.1	0.7 ± 0.1	3.9 ± 0.1
Na_2O	4.6 ± 0.2	5.8 ± 0.2	9.4 ± 0.2	3.7 ± 0.2
K_2O	4.7 ± 0.2	5.2 ± 0.2	3.0 ± 0.2	7.8 ± 0.2
Viscosity (MPa· s)	2.80	1.96	0.91	3.55
Surface tension (N m^{-1})	0.319	0.317	0.319	0.323

Table III – Physical and mechanical properties of white porcelain stoneware tiles

		C	E	N	P
Open porosity	(vol %)	0.03 ± 0.02	0.12 ± 0.06	0.09 ± 0.03	0.08 ± 0.03
Water absorption	(wt %)	0.01 ± 0.01	0.05 ± 0.02	0.09 ± 0.01	0.03 ± 0.01
Total porosity	(vol %)	3.77 ± 0.02	4.88 ± 0.03	3.39 ± 0.02	6.04 ± 0.04
Bulk density	(g cm^{-3})	2.47 ± 0.01	2.46 ± 0.01	2.48 ± 0.01	2.51 ± 0.01
Specific weight	(g cm^{-3})	2.57 ± 0.02	2.59 ± 0.02	2.59 ± 0.02	2.67 ± 0.03
3-points flexural strength	(MPa)	56.3 ± 4.3	50.7 ± 1.9	42.5 ± 3.4	48.7 ± 8.7
4-points flexural strength	(MPa)	88.4 ± 4.5	75.0 ± 1.5	76.0 ± 2.1	65.0 ± 4.1
Young modulus	(GPa)	77.0 ± 0.2	69.0 ± 0.2	72.0 ± 0.2	74.0 ± 0.2
Fracture toughness	(MPa $m^{0.5}$)	1.31 ± 0.04	1.16 ± 0.04	1.25 ± 0.04	1.14 ± 0.06
Critical defect size	(μ m)	145 ± 10	158 ± 8	179 ± 11	204 ± 24

Table IV - Tribological and functional properties of white porcelain stoneware tiles

		C	E	N	P
Average roughness (R_a)	(μ m)	0.25 ± 0.07	0.23 ± 0.08	0.32 ± 0.08	0.26 ± 0.06
Maximum depression (R_t)	(μ m)	6.28 ± 2.86	6.09 ± 2.70	8.75 ± 2.80	5.96 ± 1.77
Vickers hardness	(GPa)	6.8 ± 0.8	6.8 ± 0.6	6.2 ± 0.6	6.4 ± 0.7
Volume removed by deep abrasion	(mm^3)	116 ± 1	131 ± 3	139 ± 3	139 ± 3
Volume removed by superficial abrasion	(mm^3)	67 ± 1	71 ± 2	60 ± 1	73 ± 2
Wear rate per unit sliding distance	($mm^3\,m^{-1}$)	1.229 ± 0.016	1.347 ± 0.030	1.510 ± 0.008	1.465 ± 0.037
Apparent contact area	(mm^2)	120.0 ± 1.6	125.0 ± 2.8	127.5 ± 0.7	127.5 ± 3.2
Resistance to stains:					
Δ E (warm water)	(adim.)	0.47 ± 0.05	1.16 ± 0.10	3.74 ± 0.50	0.66 ± 0.07
Δ E (neutral detergent)	(adim.)	0.46 ± 0.05	0.73 ± 0.06	3.20 ± 0.45	0.55 ± 0.04
Δ E (alkaline detergent)	(adim.)	0.09 ± 0.01	0.27 ± 0.03	1.40 ± 0.08	0.15 ± 0.01

Table V – Elastic moduli and thermal expansion coefficients of the mineralogical phases (J. F. Shackelford and W. Halexander, Material Science and Engineering Handbook, CRC Press, 2001)

	Sample	Glass	Quartz	Mullite	Corundum	Zircon
Young modulus (GPa)		64.4	94.5	143.1	376.9	165.5
Poisson's ratio (adim.)		0.183	0.078	0.238	0.240	0.2*
Thermal expansion coefficient (MK^{-1})	C	6.0[§]	19.3	5.0	7.5	3.8
	E	6.7[§]				
	N	7.4[§]				
	P	7.3[§]				

* estimated value
[§] A. A. Appen, Dokl Akad Nauk. SSSR 69 (1949) 841-844.

Table VI – Particle stress (MPa) which crystalline phases undergo during cooling as calculated on the basis of data in Table V.

Phase	C	E	N	P
Mullite	41	66	93	89
Quartz	-370	-350	-330	-330
Corundum	-0.14	-38	-4.7	-9.4
Zircon	0.2	0.2	0.3	0.3

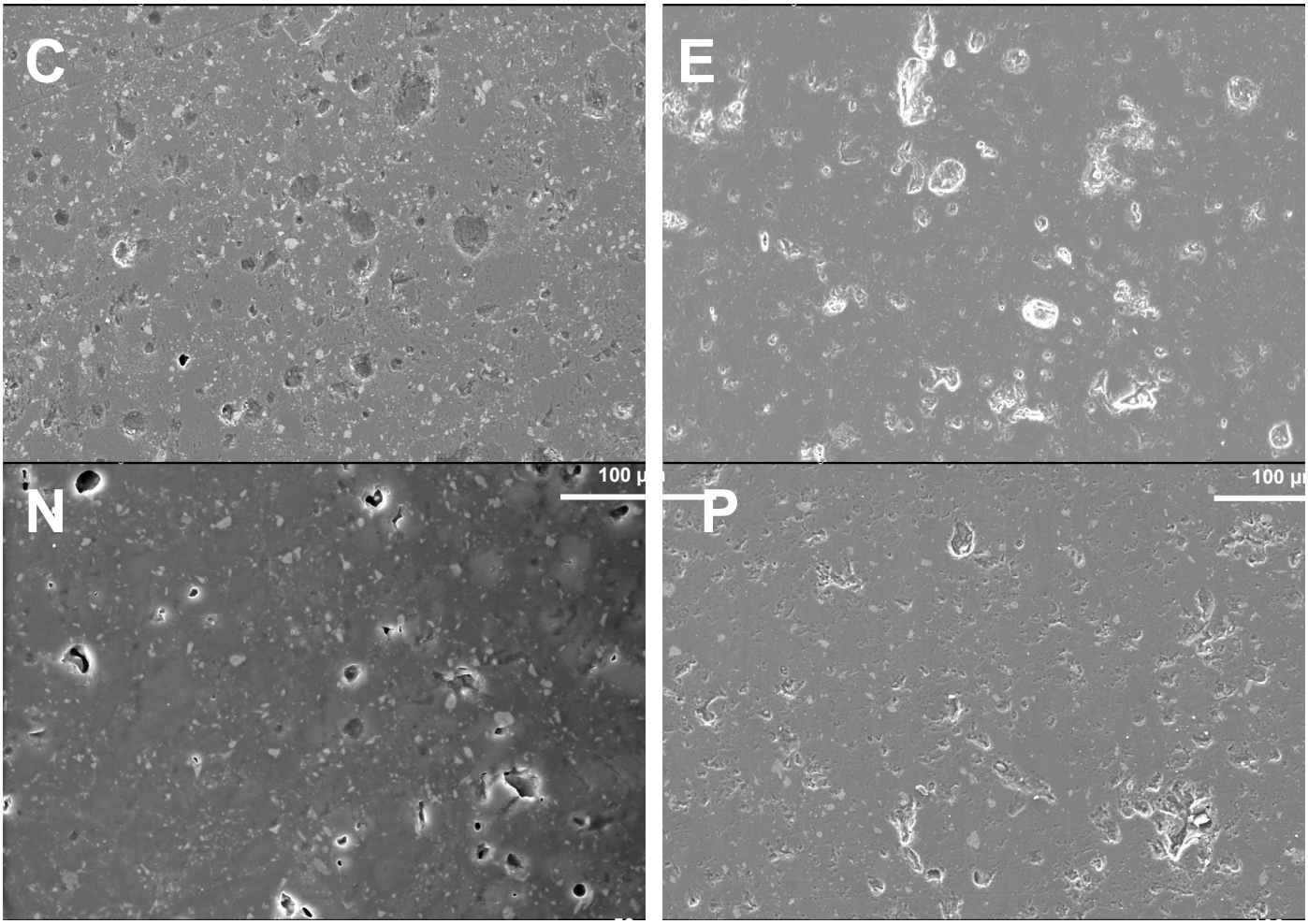

Figure 1. SEM micrographies of white porcelain stoneware tile surfaces (industrial polishing).

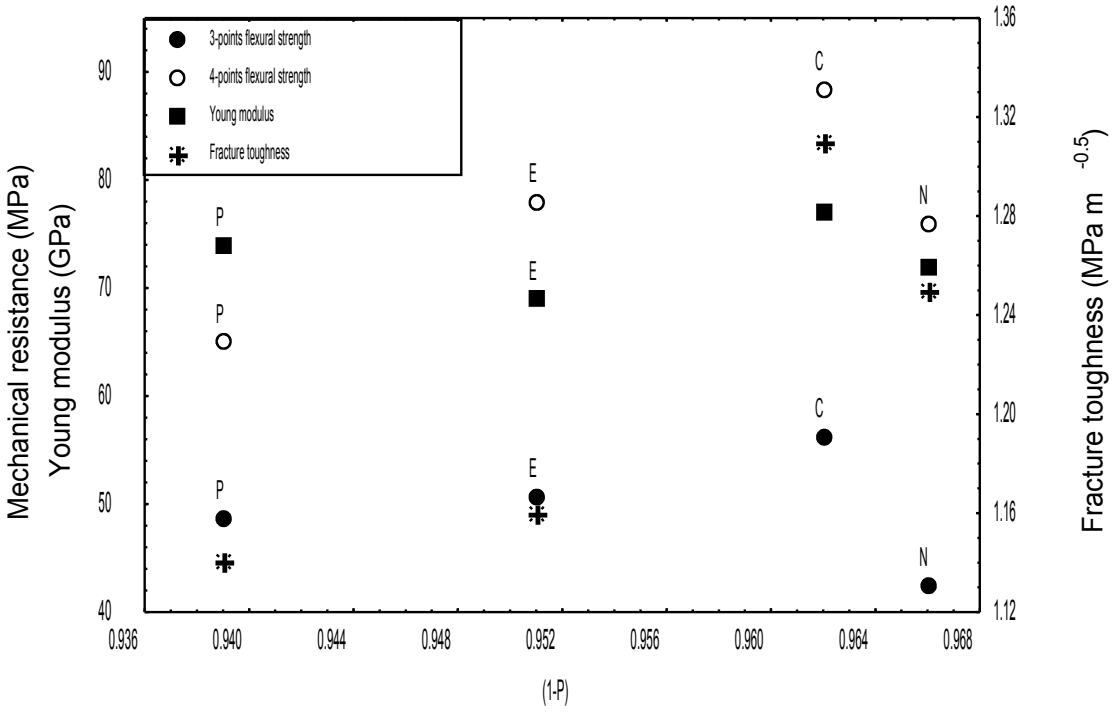

Figure 2. Dependence of mechanical properties on the porosity of white porcelain stoneware tiles.

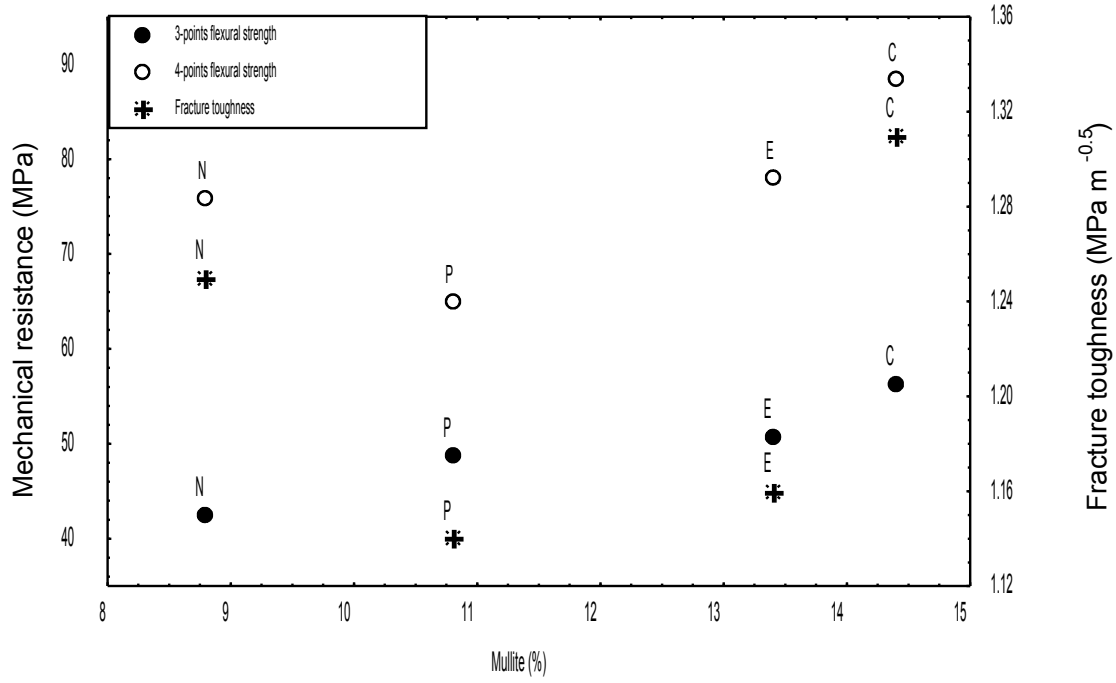

Figure 3. Relationship between mullite content and mechanical properties of white porcelain stoneware tiles.

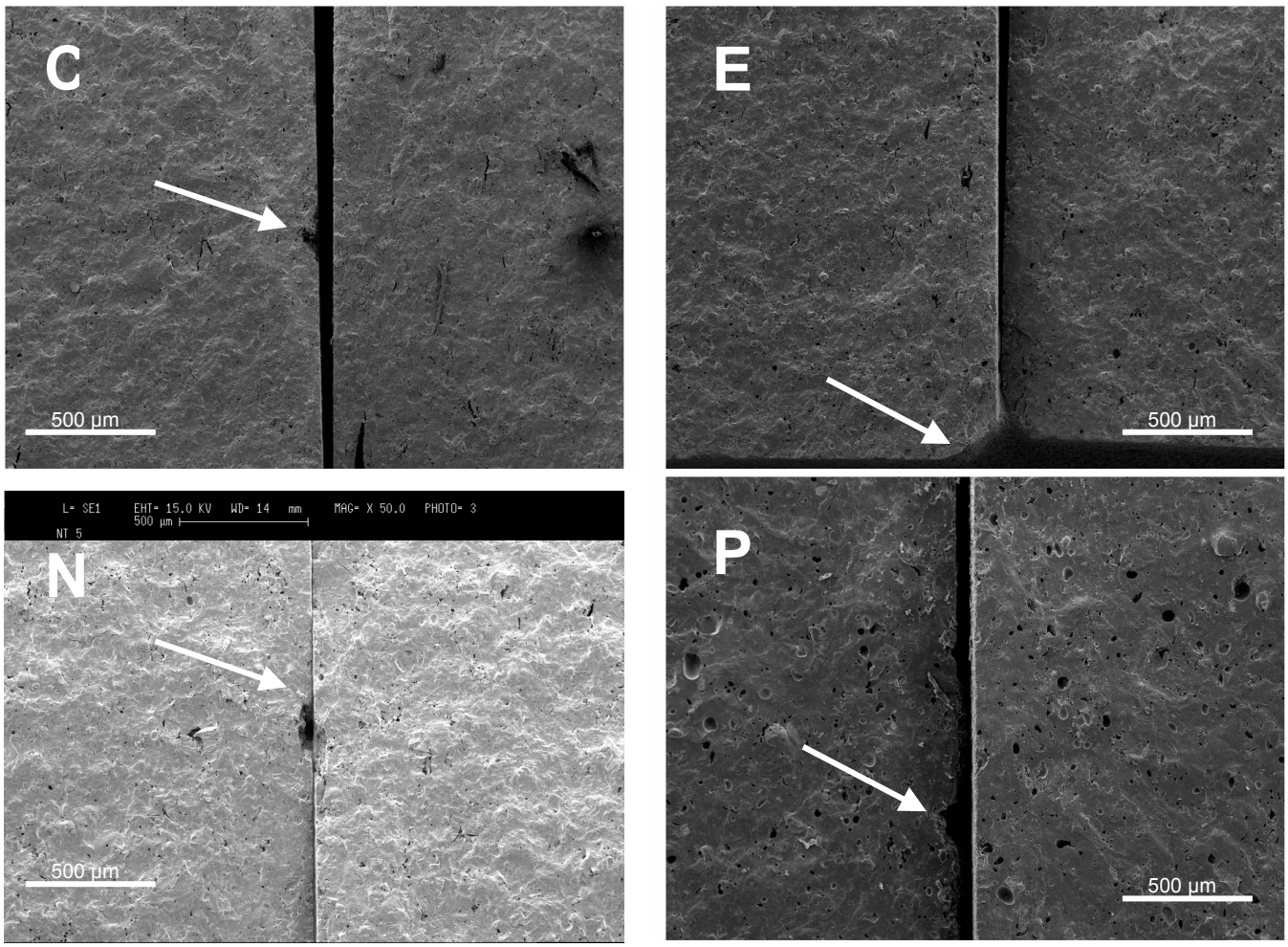

Figure 4. SEM micrographies of fracture surface after 4-points testing. Possible defects initiating the crack propagation are tentatively indicated by arrows.

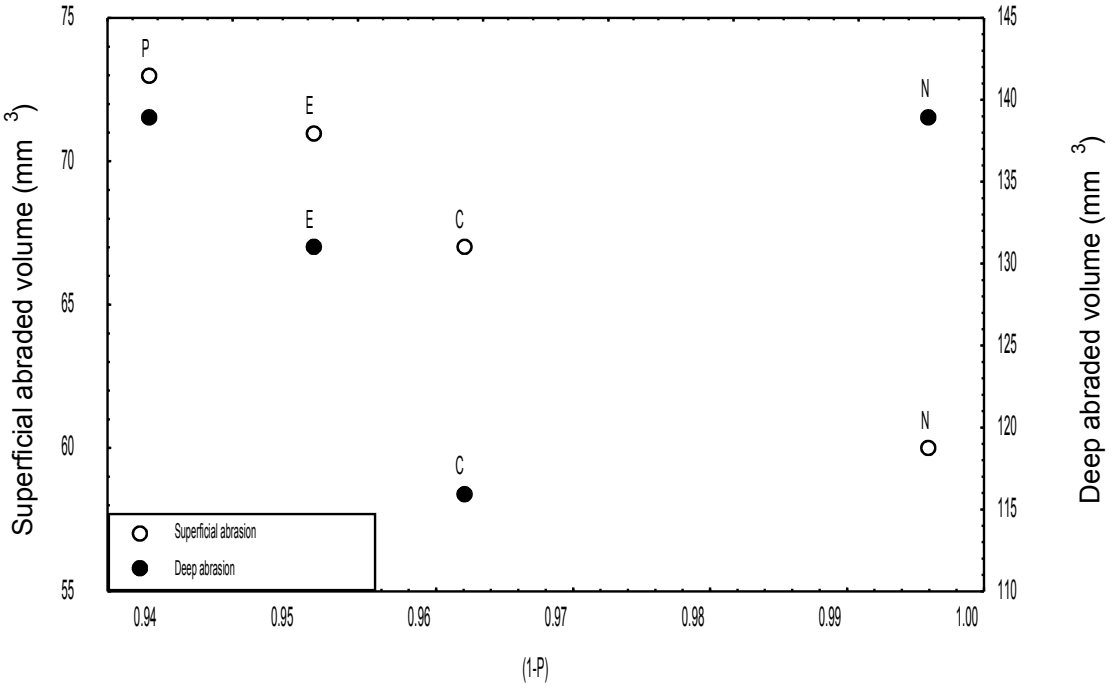

Figure 5. Dependence of the volume of material removed by superficial and deep abrasion on the porosity of white porcelain stoneware tiles.

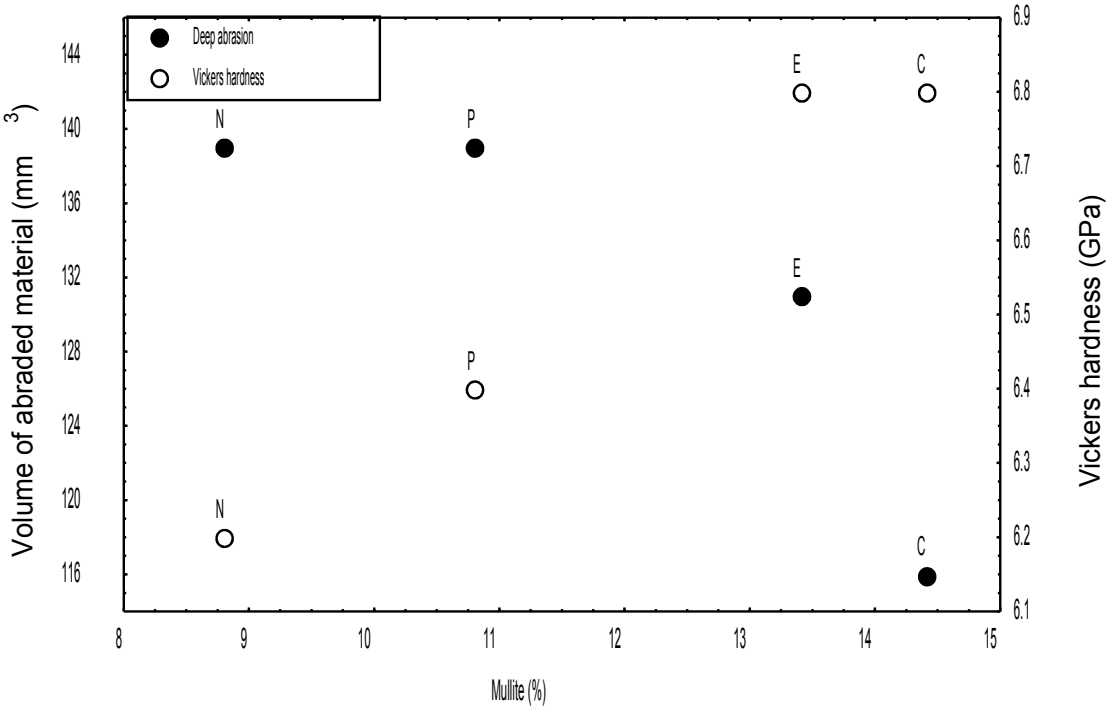

Figure 6. Dependence of the volume of material removed by deep abrasion and Vickers hardness on mullite content of white porcelain stoneware tiles.

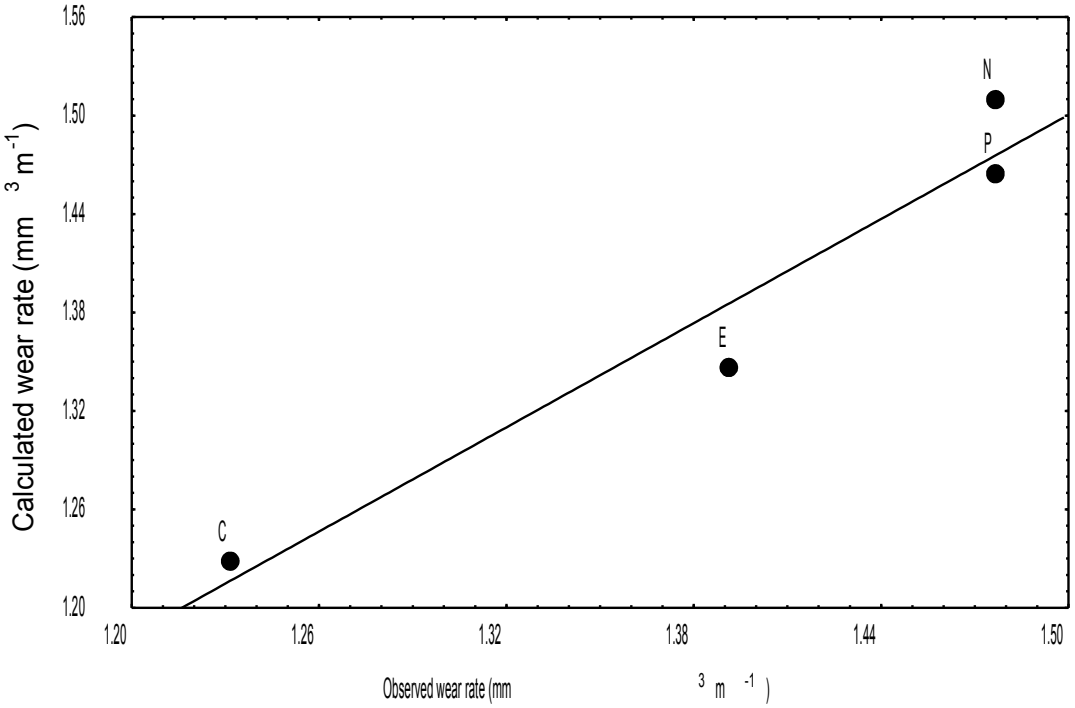

Figure 7. Calculated wear rate versus observed wear rate of porcelain stoneware tiles.

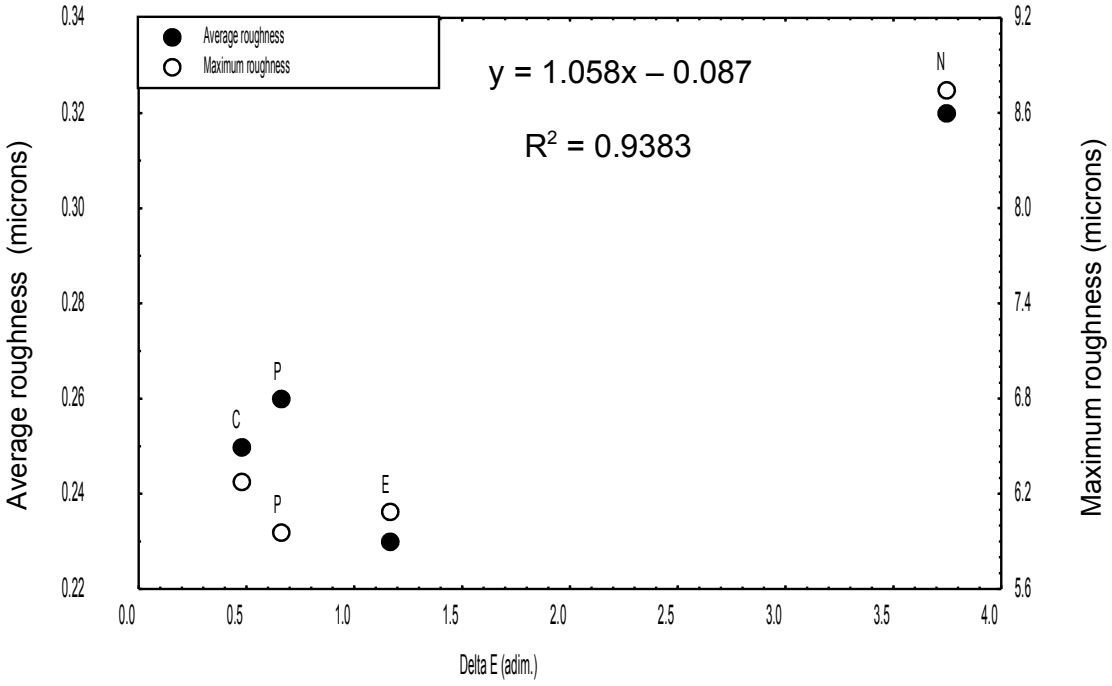

Figure 8. Dependence of Δ E values on average and maximum roughness.